TECHNICAL MEMORANDUMS

NATIONAL ADVISORY COMMITTEE FOR AERONAUTICS

No. 1044

HEAT TRANSFER OF AIRFOILS AND PLATES

By Otto Seibert

Jahrbuch 1938 der Deutschen Luftfahrtforschung

Washington
April 1943

NATIONAL ADVISORY COMMITTEE FOR AERONAUTICS

TECHNICAL MEMORANDUM NO. 1044

HEAT TRANSFER OF AIRFOILS AND PLATES*

By Otto Seibert

The few available test data on the heat dissipation
of wholly or partly heated airfoil models are compared
with the corresponding data for the flat plate as obtained
by an extension of Prandtl's momentum theory, with differ-
entiation between laminar and turbulent boundary layer
and transitional region between both, the extent and ap-
pearance of which depend upon certain critical factors.
The satisfactory agreement obtained justifies far-reach-
ing conclusions in respect to other profile forms and
arrangements of heated surface areas. The temperature
relationship of the material quantities in its effect on
the heat dissipation is discussed as far as is possible
at the present state of research, and it is shown that
the profile drag of heated wing surfaces can increase or
decrease with the temperature increase depending upon the
momentarily existent structure of the boundary layer.

INTRODUCTION

Economical high-speed flight requires aircraft of
high aerodynamic quality - that is, aircraft with air
frame designed for minimum flight drag and all parasite
areas, especially the radiators - reduced to a minimum.
In this endeavor attempts have been made in this country
as well as abroad to utilize exposed outside surfaces,
preferably those of the wings, for heat transfer. Such
radiators are hereinafter called "skin radiators."

The heat output of the exposed outside surface of a
skin radiator and its distribution across the surface are
hardly amenable to prediction from the differential equa-
tions for flow and heat exchange, as these equations are
not integrable in such generalization. However, the
moment theory and its refinement according to Prandtl af-
fords at least very satisfactory practical average values

of the heat transfer coefficients. The only stipulation
for its validity is that skin friction and heat transfer
begin and stop simultaneously. In the practical case
that some portion of the outer surface of an airplane,
whether on the fuselage, engine nacelles, or wings are
designed as skin radiator, the heat effect usually begins
after the friction; hence a temperature profile forms
progressively in the already existent and still growing
frictional boundary layer which unfortunately does not
lend itself to representation in closed form, although it
is mathematically defined by the equations of motion and
heat exchange. The correlation between the Nusselt num-
ber Nu and the Reynolds number Re for all possible
flight conditions must therefore be secured by measure-
ments on models. The subsequent study deals primarily
with the processes on wing radiators — that is, radiators
mounted in the wings. In this connection the data on
the heat dissipation of flat plates are invaluable; in-
deed, they may even save special measurements on airfoils
(see sec. V) if no unusual claims on accuracy are involved.

II. AVAILABLE TEST DATA

The most important publications on investigations
of this nature, all of which deal with wing radiators, are:

a) R.&M. Report No. 1311 (1927)
   Wind—Tunnel Tests on Gloster and Supermarine
       Wing Radiators (Supermarine airfoil section
       RAF 30, chord 15 ft = 1524 mm, model scale
       1:1, span = tunnel diameter, of which 34 in.=
       876 mm were heated, total upper and lower
       surface heatable with water separately or
       collectively).

b) R.&M. Report No. 1163 (1928)
   On the Convection of Heat from the Surface of
       an Airfoil in a Wind Current (model of RAF
       section 26, 6 in. = 152 mm chord between end
       plates at 8 in. = 203 mm spacing, with 29 span-
       wise platinum strips over the total surface).

c) R.&M. Report No. 1326 (1930)
   Wind—Tunnel Experiments on Steam Condensing
       Radiators (nose steam—heated, RAF 30 section,
       2 ft = 610 mm chord, 7 ft = 2134 mm span,

the radiator occupies 5 ft = 1524 mm; 25.1 percent of the arc length of the upper surface and 15.2 percent of the lower surface or 24 percent and 14 percent, respectively, of the chord (of the symmetrical) profile heatable with saturated vapor at low positive pressure).

d) R.& M. Report No. 1481 (1932)
    Estimation of Wing Surface Area for Evaporative Cooling (comparison of R.& M. Reports Nos. 1311 and 1326).

In figure 1 the Nusselt number $Nu = f(Re)$ is shown according to R.& M. Reports Nos. 1163, 1311, 1326, and 1481 for different angles of attack β.

where

$$Nu = \frac{\alpha_m D}{\lambda_o} = \text{Nusselt number}$$

$$Re = \frac{vD}{\nu} = \text{Reynolds number}$$

D   airfoil circumference

v   flying speed

ν kinematic viscosity referred to state of air in undisturbed zone

λ_o heat conductivity of air at surface portion.

$$t_o \sim 40^o \text{ on RAF 26,}$$

$$t_o \sim 93^o \text{ on RAF 30;}$$

Air temperature assumed at 20°.

III. CONCLUSIONS

a) The heat emissivity of the surface portions in proximity of the leading edge is greater than

at any other part of the airfoil. It naturally
increases with Re, but varies so much less
with the angle of attack β as the area ex-
tends less on the upper and lower surface.

b) On the upper and lower surface the heat dissi-
pation decreases along the wing trailing edge
for given Re; but in the transitional zone
from laminar to turbulent boundary layer it
can increase once more and then decrease, as
exemplified in the test data of R.& M. No. 1163.

c) By ascending Re and β the heat dissipation
on the upper surface increases, the function
Nu = f(Re) resembles on the whole a curve at
at least as steep as that for the nose.

d) The heat dissipation on the lower surface of the
wing scarcely varies over the practical range
of positive angles of attack; it increases at
angles of attack corresponding to zero or
negative lift. Depending upon the absolute
magnitude of Re (and other factors, see
pt. IV) the curve can be as flat as that of
the nose or about as steep as or steeper than
that of the upper surface.

While this dependence of the heat dissipation is
in general quite comprehensible, the different slopes of
the curves for the heat dissipation of the surface por-
tions cannot be summarily explained. These and other re-
lations are discussed in part IV in the light of the en-
larged momentum theory as applied to the flat plate. The
comparison of these theoretical relations with the results
obtained on the RAF 26 and RAF 30 sections (fig. 1) be-
comes particularly simple. The numerical agreement is
also very satisfactory if allowance is made for the dif-
ference in the flow velocity on the upper and lower wing
surface areas. The arguments can likewise be applied
quite satisfactorily to heated leading edges by a minor
conversion. Reliable heat dissipation data on flat plates
are available (reference 1) but they do not lend them-
selves to strict comparison with the ideal case, because
the test arrangement causes the heat dissipation to start
after the skin friction. In any event they enable to
support the theory and, in addition, afford some insight
into the expected displacements when only parts of the
wing surface area are heated. Very insufficient, however,

are the data available on the effect of the temperature
increase of the heated portion or the total surface, re-
spectively, or better, of the dimensionless surface tem-

perature $\frac{T_o}{T}$ (see pt. IV) on the heat dissipation and,

above all, on the drag of the total area. This might be
regarded as pure skin friction on the flat plate, while
on the airfoil the heating itself can influence the form
drag (pt. VII).

IV. HEAT DISSIPATION OF FLAT PLATES IN THEORY AND TEST

On real flat plates — that is, those of finite thick-
ness — the boundary layer is theoretically formed some-
what differently than on ideal plates — that is, on infinitely
thin plates in symmetrical flow parallel to its plane.
Postulating complete freedom from friction the ideal plate
does not affect the flow at all, while the real plate out-
wardly displaces the individual streamlines, depending
upon the shape of the leading edge, and so causes increases
of speed relative to the undisturbed flow.

Taking into account the skin friction, the boundary
layer on the ideal plate is produced by the decelerating
action of the surface particles on the flowing fluid which
then continues through it. Hence in two-dimensional flow
the velocity profile of a section at right angles to the
flow direction at any distance from the plate leading
edge must (as on a pipe) be unequivocally defined by the
Reynolds number (reference 2) computed with this depth   x
and the undisturbed velocity   v   and the kinematic vis-
cosity ν:

$$Rex = \frac{vx}{\nu} \qquad\qquad (1)$$

regardless of whether and how far the plate extends down-
stream. On the real plate this skin friction is superposed
by the displacement process associated with the shape of
the body (especially its thickness, over-all length, round-
ings) which very likely can also become effective upstream.
The combined action of this profile effect and the friction
favors the creation of the so-called form resistances which
cannot occur on the ideal plate.

The velocity field on the real plate must accordingly have a somewhat different aspect, which is, that the discrepancies from the theory are especially great at the beginning of the plate. The effect of the leading edge on the heat transfer is obviously similar. The foregoing logically applies also to airfoils with and without angle of setting, where an even somewhat poorer agreement is to be expected.

On ideal plates and on real thin plates* (with sharpened edge and interference-free inflow) a laminar flow forms first in the boundary layer. Turbulence does not come into being until after traversing a certain entrance length x_{cr} which can be computed from the so-called critical Reynolds number.

$$Rex_{cr} = \frac{vx_{cr}}{\nu} \qquad (2)$$

For $x > x_{cr}$ the laminar boundary layer becomes fully turbulent in a transitional region; Rex_{cr} according to Ten Bosch (reference 2, pp. 139-140), has been measured up to 5×10^5 for very small initial disturbances, but may drop to 10^5 in the presence of major disturbances, the transitional region can extend from $Rex = 10^5$ to 2×10^7 for sharpened edge and steadied flow. With the one-sided surface C of the plate, the drag coefficient C_f and the air density ρ the drag of the ideal plate W for each side is

$$W = C_f O \frac{v^2 \rho}{2} \qquad (3)$$

The amount of heat dissipation from one side of the plate at increase of temperature ϑ

$$Q = \alpha_{m K} O \vartheta \qquad (4)$$

is, according to simple momentum theory, and as employed by Von Kármán and Latzko (references 3 and 4), to the

_____

*Thus Ten Bosch (reference 2) indicates on page 148 that heat exchange surface of streamline form should have less than $33 \times 100/600 = 5.5$ percent profile thickness, since only from this slenderness ratio on the friction forms the principal portion of the total drag. (See also pp.139-140.)

plate drag as the heat content of some gas mass in the nucleus to its quantity of motion:

$$\frac{Q}{W} = \frac{(\rho v)(g\,c_{pm}\,\vartheta)}{(\rho v)v} = \frac{g\,c_{pm}\vartheta}{v} \qquad (5)$$

Equations (3), (4), and (5) afford

$$\alpha_{mK} = \frac{Q}{W}\,\frac{W}{O\vartheta} = \frac{1}{2}\,C_f c_{pm}\,v\,\gamma \qquad (6)$$

or the mean Nusselt number with the plate chord x introduced in equation (1):

$$Nux_x = \frac{1}{2}\,C_f\left(\frac{g\,c_{pm}\,\eta}{\lambda}\right)\left(\frac{v\,x\,\rho}{\eta}\right) = C_f\,\frac{1}{2}\,Pr\,Rex \qquad (7)$$

A similar line of reasoning was originally followed by O. Reynolds (reference 5) to the flow in circular pipes. But here, as on the flat plate, this simple theorem enables a satisfactory reproduction of the actual amount of heat transfer only in the specific case where the Prandtl number

$$Pr = \frac{g\,\eta\,c_p}{\lambda}$$

is equal to unity. In all practical cases for which $Pr \neq 1$; hence for air also,* divergencies are found which Prandtl attempts to comply with by assuming a special gas film between surface and actual boundary layer within which the gas velocity increases in proportion to the wall distance. Its thickness and velocity distribution existing in it are defined by the proportionality factors ψ and φ, to be computed from experiments (reference 2). Hence, according to the enlarged Prandtl equation:

$$\alpha_m = \frac{\frac{1}{2}\,C_f c_{pm}\,v\,\gamma}{\psi - \varphi(1-Pr_g)} \qquad (8)$$

---

*$Pr \sim 0.725$ for air of surrounding temperature; Pr varies only slightly with temperature.

$$Nux = \frac{\frac{1}{2} C_f}{\psi - \varphi (1 - Pr_g)} \frac{c_{pm} \gamma_{vx}}{\lambda} = C_f \frac{\frac{1}{2} Pr}{\psi - \varphi(1 - Pr_g)} Rex \qquad (9)$$

with Pr_g indicating the Prandtl number for the "<u>bound-ary layer temperature</u>." Prandtl gives the values ψ and φ only for the round pipe. In the case of

heating of the fluid $\psi = 1 \quad \varphi = 1.4 \quad Pr^{-0.185} Re^{-0.1}$

cooling of the fluid $\psi = 1 \quad \varphi = 1.12 \quad Pr^{-0.185} Re^{-0.1}$

and in both cases $Re = \dfrac{vd}{v} \quad d =$ pipe diameter

Ten Bosch computed $\psi = 0.89$ and $\varphi = 1.4 \, Pr^{-0.185} Rex^{-0.075}$ from experiments for the flat plate. The heat transfer factor is further dependent upon the difference Θ between surface temperature and gas temperature. Ten Bosch assumes a <u>turbulence variation</u>, ξ as factor in the drag coefficients. Lacking more precise data he gives quantity ξ as function of the increase of temperature Θ. Figure 2 holds true for flow in round pipes. Ten Bosch further suspects a probably minor dependence on Pr. For a more exact exploration of these important interconnections the author recommends in place of Θ two variables: the absolute temperature T of the gas and the ratio T_g/T — that is, the "dimensionless" boundary layer temperature — where T_g is the mean absolute temperature of the boundary layer.

If, as in the present case, only one gas is involved, the absolute wall temperature T_w may be substituted for T_g as determining quantity, and Pr discounted; Θ is positive for heating of the air.

Since the dependence $\xi = f(\Theta)$ for the flat plate is not known, figure 2 will serve as a basis within the framework of the present report.

In relation to equation (7), equation (9) contains the <u>improvement</u> factor

$$V = \frac{1}{\psi - \varphi (1 - Pr_g)} \qquad (10)$$

which for constant Pr and Pr_g can be represented as (slightly variable) power function of Rex (cf. equation (18)).

The equations for C_f', α_m, and Nux in the three zones:

a) In Laminar Boundary Layer (Subscript L):

For isothermic flow

$$C_{fLis} = 1.328 \; Rex^{-0.5}$$

for any increase of plate temperature

$$C_{fL} = 1.328 \; \xi_L \; Rex^{-0.5} \qquad (11)$$

with equation (11) and the simplification through $Pr_g = 1$ in equation (8), we get

$$\alpha_m = \frac{1.328 \; \xi_L \; Rex^{-0.5}}{2} \; \frac{v \, c_{pm} \, \gamma}{\psi} = \frac{0.664}{\psi} \; \xi_L \; \lambda \; \frac{Pr}{x} \; \sqrt{Rex}$$

against the approximation according to theoretical solution conformably to E. Pohlhausen (reference 2, p.144)

$$\alpha_o x = \frac{0.664 \lambda}{x} \; \frac{\Theta_1}{\Theta_m} \; \sqrt[3]{Pr} \; \sqrt{Rex}$$

For the completely free plate, $\dfrac{\Theta_1}{\Theta_m} = 1$; ψ is unknown in the first equation, and, although the term $\sqrt[3]{Pr}$ in the second equation represents an approximation the reliability of which is limited to the range of $Pr = 1000$, it is nevertheless used for air. Besides, both equations become identical for $\psi = 1$, $\xi_L = 1$ and $Pr = 1$. Experiment alone can indicate which relation comes closest to reality. A variation of the "turbulence" in the laminar boundary layer owing to finite increase of temperature is to be disregarded. It might be assumed that ξ becomes less than 1 for heating (positive Θ), as in turbulent flow in pipes, and greater than 1 for cooling.

Henceforth:

$$Nux_L = \frac{1}{2} \; C_f \; \sqrt[3]{Pr} \; Rex^{0.5}, \; Pr \sim 0.725, \; \frac{1}{2} \sqrt[3]{Pr} = 0.449 \qquad (12)$$

b) Transitional Region in Boundary Layer
(Subscript Ü)

According to an approximation by Prandtl the drag coefficient of the total plate for Rex between 5×10^5 and 2×10^7 — ξ allows for the increase of temperature — is

$$C_{fPr} = \left(\frac{0.455}{(\log Rex)^{2.58}} - 1700\, Rex^{-1}\right)\xi \qquad (13)$$

The figure 1700 is merely the mean value for a range within which the true value can fluctuate, depending upon the initial disturbances.* Although all important conclusions could be drawn from the variable slope of this curve from its lower limit of validity $(Rex \sim 5\times10^5)$, an approximation by Ten Bosch is introduced which, while not quite as close, has the advantage of bringing out the effect of Rex_{cr} on the drag coefficient and naturally also on the heat dissipation.

The total frictional drag is visualized as being composed of the forward plate portion L on which the boundary layer is laminar, and of the rest of the plate portion Ü, along which the boundary layer transforms, whereby the latter portion might be put at

$$C_{f\ddot{U}} = 0.003 \qquad (14)$$

independent of Rex. With equation (10) we get in this instance:

$$Nux_{\ddot{U}} = \frac{\frac{1}{2} C_{f\ddot{U}}\, Pr}{\psi - \varphi(1 - Pr_g)}\, Rex = C_{f\ddot{U}}\, V\, \frac{1}{2}\, Pr\, Rex \qquad (15)$$

c) Turbulent Boundary Layer (Subscript T):

For $Rex > 2\times10^7$

---

*Ten Bosch used an older form giving almost the same values as equation (13), the first term of which reads $0.072\, Rex^{-0.2}$ For further information on the drag coefficients of flat plates at large Reynolds numbers see reference 6.

$$C_{fT} = 0.072 \, \xi \, Rex^{-0.2} \tag{16}$$

$$Nux_T = \frac{\frac{1}{2} \, C_{fT} \, Pr}{\psi - \varphi \, (1 - Pr_g)} \, Rex = C_{fT} \, V \, \frac{1}{2} \, Pr \, Rex \tag{17}$$

By observance of the above values for ψ and φ and approximation $Pr \sim Pr_g$, the improvement factor according to equation (10) becomes

$$V \sim 1.36 \qquad \text{for} \quad Rex = 5 \times 10^5$$

$$V \sim 1.30 \qquad \text{for} \quad Rex = 10^7$$

or, represented as power function:

$$V = \frac{1.638}{\sqrt[70]{Rex}} = 1.638 \, Rex^{-0.0143} \tag{18}$$

This relation needs to be checked by accurate tests and improved accordingly.

Figure 3 shows the drag coefficients C_f according to equations (11), (13), (14), and (16) and the mean Nusselt number Nux over the range $Rex = 2.5 \times 10^4$ to 1.5×10^7 for the unheated plate. Posting the respective term for C_f and of V in Nux according to equation (18) (again for $\Theta = 0$) affords

a) for the laminar boundary layer according to equation (12)

$$Nux_L = 1.328 \times 0.449 \, Rex^{0.5} = 0.597 \, Rex^{0.5}$$

b) for the transitional region according to equation (15):

$$Nux_{\ddot{U}} = 0.003 \times 1.638 \times 0.3625 \, Rex^{0.9857}$$
$$= 0.00178 \, Rex^{0.9857}$$

or, according to Prandtl,

$$Nux_{Pr} = \frac{0.455 \times 1.638 \times 0.3625 \, Rex^{0.9857}}{(\log Rex)^{2.58}}$$
$$- 1700 \times 1.638 \times 0.3625 \, Rex^{-0.0143}$$

$$Nux_{Pr} = 0.27 \frac{Rex^{0.9857}}{(\log Rex)^{0.258}} - 1010 \, Rex^{-0.0143}$$

c) for the turbulent boundary layer according to equation (17)

$$Nux_T = 0.072 \times 1.638 \times 0.3625 \, Rex^{0.7857}$$
$$= 0.0428 \, Rex^{0.7857}$$

according to equation (7):

$$Nux_K = 0.072 \times 0.3625 \, Rex^{0.8} = 0.0261 \, Rex^{0.8}$$

(19)

For easier plotting of the individual theoretical lines figure 3 contains several numerical values following from these equations.

The reason for the choice of the specific case of infinitely small increase of temperature on the plate surface was the avoidance of uncertainty in the choice of ξ which in this instance become equal to 1. The drag coefficient of plates with finite increeae of temperature is theoretically analyzed in part VII. For $Rex < Rex_{cr}$

$$C_f = C_{fL}; \quad Nux = Nux_L$$

For $Rex > Rex_{cr}$ up to the end of the transitional region (at $Rex \sim 2 \times 10^7$), the mean values are:

$$C_f = \frac{C_{fL[Rexcr]} \, Rexcr + C_{f\ddot{U}} (Rex - Rexcr)}{Rex}$$

$$= (C_{fL[Rexcr]} - C_{f\ddot{U}}) \frac{Rexcr}{Rex} + C_{f\ddot{U}}$$

$$Nux = \frac{Nux_{L[Rexcr]} \, Rexcr + Nux_{\ddot{U}} (Rex - Rexcr)}{Rex}$$

$$= (Nux_{L[Rexcr]} - Nux_{\ddot{U}}) \frac{Rexcr}{Rex} + Nux_{\ddot{U}}$$

whereby the length ratio $\dfrac{x_{cr}}{x}$ is at the same time replaced by $\dfrac{Rex_{cr}}{Rex}$. The two cases

$$Rex_{cr} = 10^5 \quad \text{and} \quad Rex_{cr} = 5 \times 10^5$$

are differentiated.

On plates of such total depth x that Rex ranges between 10^5 and $\sim 2 \times 10^6$, C_f and Nux values situated in the shaded region should be possible to be measured (up to ± 40 percent referred to some mean value). (See reference 7.) For still greater plate depths the uncertainty decreases then rapidly (figure 3). Prandtl's formula gives a curve similar to that of the linear composition under the assumption of especially great freedom from disturbance.

The heat dissipation (and the temperature and velocity fields) of a flat plate have been treated in detail by Elias (reference 1). The plate was 500 millimeters deep, 250 millimeters wide and 29 millimeters thick with a wooden frame around it. The strip facing the flow was $x_1 = 100$ millimeters deep and carefully tapered for the purpose of minimizing the initial disturbances. Referring the heat volume Q, dissipated from both sides up to a certain depth x, to the unit span, he plotted the (named) term $\dfrac{Q}{\vartheta\, xv}$ against Rex (or Pex). This is then compared with the theoretical value $\dfrac{1}{2}\, C_f c_{pm}\gamma$ following from equation (6). The displacement of the start of heat dissipation relative to that of friction he attempted to account for by measuring the depth of the respective section, first, from the beginning of the thermal reaction as x_{th} and then from the beginning of the hydrodynamic reaction as x_h. But neither of the representations is really able to give a satisfactory reproduction of the process.

On the other hand, the reasoning on the basis of the following is very informative despite the marked scatter: if the plate had been heatable up to the leading edge it would naturally have dissipated more heat by reason of its larger area and the added existence of a region of strong transformation of the velocity profile and hence of best heat dissipation. In the dimensionless representation

the upper limit value Nux_{max} theoretically corresponds to the curves Nux according to equation (19). The actually heated portion would, of course, have then been able to dissipate less heat than in the experiment; namely,

$$
\left.
\begin{aligned}
Nux_{min} &= \frac{Nux_{(x=x)}\; x - Nux_{(x=x_1)}\; x_1}{x} \\
&= Nux_{(x=x)} - Nux_{(x=x_1)}\; \frac{x_1}{x} \\
&= Nux_{(x=x)} - Nux_{(x=x_1)}\; \frac{Rex_{(x=x_1)}}{Rex_{(x=x)}}
\end{aligned}
\right\} \quad (20)
$$

The measured heat or its corresponding Nux_m must lie between these two limits.

For comparison with the test data of Nux_m, the value Nux_T is used in figure 4.

For a constant x_1/x equation (20) becomes

$$
\left.
\begin{aligned}
Nux_{min} &= 0.0428\; Rex_{(x=x)}^{0.7857} - 0.0428 \left(\frac{x_1}{x} Rex\right)_{(x=x)}^{0.7857} \frac{x_1}{x} \\
&= 0.0428\; Rex_{(x=x)}^{0.7857} \left[1 - \left(\frac{x_1}{x}\right)^{1.7857}\right] \\
&= Nux_{T(x=x)} \left[1 - \left(\frac{x_1}{x}\right)^{1.7857}\right]
\end{aligned}
\right\} \quad (21)
$$

The factor w - that is, the ratio of the actual mean Nusselt number referred to that of the total depth

$$
w = \frac{Nux_m}{Nux_T} \qquad (22)
$$

therefore ranges between $1 - \left(\frac{x_1}{x}\right)^{1.7857}$ and 1. The parameters are $x_1/x = 1/2,\ 1/3,\ 1/4,$ and $1/5$, each of which is applicable to one plate each with a "cold" forward and a "hot" residual portion amounting to 2, 3, 4, and 5 times that of the front portion each in a different airspeed flow v (between 10 and 35 m/s). It is readily seen that,

(a) With exception of the range of small Reynolds numbers the Nux_m are located above the Nux_K, as anticipated.

(b) The experimental curves (and the w factors) are located between the theoretical limiting values.

(c) They are, admittedly, not quite so systematically staggered according to parameter as equation (21) postulates.

(d) With increasing Re_x they approach, contrary to equation (21), the curve of Nux_T - that is, the factor w depends on Re_x owing to the dissimilarity of correlated velocity and temperature fields.

(e) The marked steepness of the actual Nux curves from the beginning indicates that the critical Reynolds number according to equation (2) is close to the lower limit 10^5.

In this comparison, especially for point (d), it should be noted that the function Nux_T is not as yet completely defined as to magnitude and steepness. Systematic discrepancies in figure 4, which would have to be interpreted as temperature effect, are, of course, not discernible by reason of the smallness of the chosen Θ.

V. APPLICATION TO AIRFOILS

These studies on the heat dissipation of flat plates can be applied to airfoils. It is advisable to treat the upper and lower surfaces separately by introducing as characteristic length x the measured distance around the airfoil from the stagnation point, the "start" of the boundary layer, up to the end of the heated area.

By reason of the variation of the airspeed along the airfoil circumference as a result of the angle of attack and of the finite airfoil thickness, individual mean velocities v_x for upper and lower surfaces must be introduced, which follow from the undisturbed velocity, say, with the aid of the mean differences Δp of the static pressures on both sides of the airfoil in ratio to the dynamic pressure $q = \dfrac{v^2\rho}{2}$. The mean Δp values are

obtainable from pressure distribution curves. Assuming
that the acceleration or deceleration follows Bernoulli's
equation, we get (for constant air density ρ):

$$\left.\begin{array}{c} \dfrac{v_x^2\rho}{2} - \dfrac{v^2\rho}{2} = \Delta p \\[3mm] \left(\dfrac{v_x}{v}\right)^2 = 1 + \dfrac{\Delta p}{q} \end{array}\right\} \qquad (23)$$

$\dfrac{\Delta p}{q}$ is, of course, posted with its algebraic value (nega-
tive for the lower surface at positive lift).

    For simplification the slight travel of the stagna-
tion point with the angle of attack and the identical
absolute variations of the lengths x are discounted.
The pressure distribution need not be known, if satisfied
with the admittedly very rough approximation that the
velocity on the wing upper surface is greater by the
amount Δv meters per second, and on the lower surface
smaller by the same amount than the undisturbed flow
velocity v. Actually, local velocities amounting to
multiples of the undisturbed flow prevail on the forward
portion of the upper surface especially on thick and high
incidence airfoils, while the decelerations on the lower
surface are substantially less. On the other hand,

$$\left[(v + \Delta v)^2 \frac{\rho}{2} - v^2 \frac{\rho}{2}\right] + \left[v^2 \frac{\rho}{2} - (v - \Delta v)^2 \frac{\rho}{2}\right] = \Sigma \Delta p$$

$$4 v \Delta v \frac{\rho}{2} = \Sigma \Delta p$$

where $\Sigma \Delta p$ denotes the mean pressure difference between
upper and lower surfaces. With wing area F and angle
of attack β we get

$$\left.\begin{array}{c} c_a F v^2 \dfrac{\rho}{2} = F \Sigma \Delta p \cos \beta \\[3mm] \Delta p = \dfrac{c_a}{\cos \beta} v^2 \dfrac{\rho}{2} \\[3mm] \dfrac{\Delta v}{v} = \dfrac{c_a}{4 \cos \beta} \\[3mm] \dfrac{v_x}{v} \sim 1 \pm \dfrac{c_a}{4 \cos \beta} \end{array}\right\} \qquad (24)$$

For normal angles of attack cos β = 1. The functions
v_x/v are shown plotted against c_a in figure 5.

The Reynolds number used in the following is obtained
from the Re employed in figure 1, by correction of the
velocity from $\cdot v$ to v_x according to equation (23) or
approximation (24) and replacement of profile circumfer—
ence D by chord x measured on the circumference:

$$Re_x = Re \; \frac{v_x}{v} \; \frac{x}{D} \qquad\qquad (25)$$

The conversion of the Nusselt number is simpler

$$Nu_x = Nu \; \frac{x}{D} \qquad\qquad (26)$$

In figure 6 the association of figures 1 and 3 with the
factors of equations (25) and (26) for the flat plate and
the two airfoils is compared. It is to be noted that the
transition from v to v_x shifts the points horizontally,
the transition from D to x in the direction 1:1.

On RAF section 26 and RAF section 30 x/D is assumed
equal to 1/2 for upper and lower surfaces. The values for
the nose on both airfoils are plotted on the assumption
that the undisturbed velocity v as located between the
two v_x is more suitable; x/D is averaged at 0.20 for
both sides of the wing. The curves in figure 6 cover the
test range of figure 1 from beginning to end.

In the comparison it is to be noted that a different
temperature t_o or increase of temperature Θ is applied
to each of the three cases:

	t_o	Θ
RAF 26 . .	~40°	~20°
RAF 30 . .	~93°	~73°
Flat plate	Air temperature	0°

The fully heated models manifest the following:

a) All straight lines lie practically within the
zone bounded by the theoretical curves Nux_L,
Nux_U, Nux_T applicable to the flat plate.

b) On both airfoils the straights representing the
heat dissipation of the upper surface at dif-
ferent angles of attack are packed closer
together, those for the lower surface a little
farther apart.

c) In conformity with the "narrowness" of the zone
for large Rex on the (symmetrical) RAF 30 sec-
tion the systems of curves for both sides of
the wing fall especially close together at
equal angle of attack.

d) The slope of the separate straights for the RAF
26 section (with exception of those for $U\beta - 0.9°$)
rises fairly uniformly with increasing distance
from Nux_L and ultimately approaches that of
Nux_T.

e) The laminar boundary layer persists for some time
on the lower surface, but the curve for the
Rex factors above the upper limit of the test
range for RAF 26 section appears to become
steeper and, as theoretically stipulated, hugs
the straight Nux_U until it deflects toward
Nux_T in the range of the factors of the RAF 30.

Heated wing leading edge:

f) Here the accord with theory is not so good as already
indicated. The deciding velocity is nevertheless
very much dependent on the angle of attack as
reflected by the fairly great distance between
the straights on both airfoils corresponding to
the lift coefficients ~0.24 and 0.64. Added
to this is the effect of especially high in-
creases of velocity in this region. The heat
dissipation of the nose portion on the upper and
lower surfaces of the RAF 26 section could also
be computed separately from the quoted data (pt.
II) and evaluated in the discussed manner, where-
by the pressure distribution might afford even
"better" velocities v_x and perhaps even better
arc lengths x by reference to the respective
stagnation point.

From d) it can be concluded that the boundary layer
on the wing upper surface changes sooner and becomes fully
turbulent quicker than expected according to the value of
Rex computed with $v + \Delta v$. Undoubtedly this is accom-
plished by the cited increases of velocity to which larger
Reynolds numbers also correspond. The total surface area
of the RAF 26 model is "rough" by reason of the glued-on
platinum strips and it is surprising that the boundary
layer remains laminar over the greater part of the lower
surface, as indicated quite plainly by the location of the
respective straight lines. However, the more scattered
test values for $U\beta - 0.9°$ allow it to be inferred that
the laminar boundary layer is no longer stable even at low
angles of attack and lift coefficients, respectively — that
is, even for very small differences relative to the flow
velocity. According to the foregoing it may be expected
that in the range of $Rex << 10^5$ the laminar boundary
layer on the upper surface also extends over continuously
greater depths with decreasing Rex, so that the curves
Nux become progressively flatter (reference 2, p. 153).
The S-shape course is naturally less pronounced on the
curves for the wing upper surface than on those for the
lower, because they are of themselves quite close to the
asymptote Nux_T for maximum Rex.

VI. CHOICE OF MATERIAL QUANTITIES

The studies described under part IIa) to d) were made
on rectangular model airfoils (up to scale 1:1) of great
aspect ratio, only a small portion of the span being used
as heating surface, or on such between end plates (two-
dimensional flow closely approximated in both cases). The
airfoil circumference D serving as characteristic length,
was little more than twice the wing chord.

The material values λ and η involved in the dimen-
sionless factors are related to the temperature (about pro-
portional to $\sqrt{T}$). In none of the practically important
cases of heat-transfer (flow in pipe, flow around pipe, flat
plate) has there, up to now, been successfully determined a
"decisive mean temperature" dependent on surface tempera-
ture, gas temperature, Reynolds number (and Prandtl number)
to which the material values were to be referred. In R.&M.
Reports Nos. 1326 and 1481 the Reynolds number Re is com-
puted with the kinematic viscosity v for outside air

temperature t. In Nu, λ is introduced with the value
corresponding to that of the surface temperature t_0,
since the processes in the boundary layer are justly held
as the essential. .When, furthermore, Ten Bosch recommends
the kinematic viscosity $\nu = \eta/\rho$ corresponding to the
surface temperature for the plate in forced flow even in
Rex, since as proved by experiment, it was best "suitable"
for the plate in free flow, this procedure should answer
the purpose for airfoils as well. It would involve the
conversion of the "aerodynamic" Rex to the "thermic" Rex_0.

$$Rex_0 = Rex \left(\frac{\rho_0/\eta_0}{\rho/\eta} \right) = Rex \; \frac{T \eta}{T_0 \eta_0} \qquad (27)$$

The conversion factor $U_{Rex \rightarrow Rex_0} = \dfrac{T \eta}{T_0 \eta_0}$ is simply a

function of the two temperatures t and t_0 (if this is
variable a mean value substitutes). To avoid confusion
between Rex and Rex_0 it would be preferable to use the
respective Péclet number $Pex_0 = Pr_0 Rex_0$ in place of Rex_0,
the Prandtl number Pr may be averaged at ~0.725. The

conversion factor $U_{Rex \rightarrow Pex_0} = 0.725 \; \dfrac{T \eta}{T_0 \eta_0}$ also depends

on t and t_0 only. Accordingly, if the temperature ef-
fect is taken into account, all straight lines of figure 6
relating to the airfoils shift toward the left, while Rex
remains $= Rex_0$ for the flat plate. But the Nusselt number
for the flat plate must be multiplied by the still unknown
factor ξ . Assuming that it is smaller than 1 for the case
of a heat dissipating surface similar to the flow through
a pipe, the curves must shift downward with rising plate
temperature and the close agreement of figure 6 is complete-
ly lost.

It would afford for the

$$RAF \; 26 \quad t_0 = 40^0$$
$$t = 20^0$$

$$U_{Rex \rightarrow Pex} = 0.725 \; \frac{273 + 20}{273 + 40} \times \frac{1.86}{1.95} = 0.647$$

and for the

$$RAF \; 30 \quad t_0 = 93^0$$
$$t = 20^0$$

$$U_{Rex \rightarrow Pex_0} = 0.725 \; \frac{273 + 20}{273 + 93} \times \frac{1.86}{2.18} = 0.495$$

Accepting, in the absence of other data, the correlation of ξ with the increase of temperature of the pipe for the flat plate, the surface temperature becomes

$$t_o = 40^\circ \quad \Theta = 20^\circ \quad \xi = 0.92; \quad t_o = 93^\circ \quad \Theta = 40^\circ \quad \xi = 0.88$$

$$UR_{ex} \longrightarrow P_{ex_o} = Pr = 0.725$$

The result is illustrated in figure 7. The percentage of discrepancies between the experimental and theoretical data is readily apparent. They amount to more than 60 percent (on the RAF 30 section). Accordingly, it is very question-able whether Ten Bosch's suggested method actually repro-duces the true conditions; in any event it would not ex-plain what effects the theoretical values for the heat dissipation on the recorded, are able to increase. It fur-thermore conflicts with the view that the formation of the major portion of the boundary layer proceeds the same as in isothermic flow, the absolute temperature of which is, however, T_o rather than T. The effect is therefore much too great.

In any case the arguments seem to indicate that the temperature effect for every one of the three boundary layer structures involved is of a different nature. Ex-periments in this zone will require care to assure laminar boundary layer over the entire depth of the airfoil or plate, and then to secure a turbulent boundary layer on the major part of the surface by using surfaces of maxi-mum depth (with purposely great initial disturbance (ref-erence 7). In both cases the material values of the un-disturbed flow will be introduced in the factors for the evaluation (for λ also!). The plotting of the curves $Nu_x = f(Re_x)$ with the "temperature effect" as parameter affords a formula represented in the form $(T_o/T)^n$ if limited to a gas (air), whereby the exponent n_L for laminar boundary layer need not be equal to the exponent n_T for fully turbulent boundary layer. Both will be very much smaller than 1. It might even be possible to split these powers wholly or in part in factors and to correlate them with the material values in such a way that these could be coordinated with the afore-mentioned controlling mean temperature, as has been accomplished for horizon-tal wires and pipes to a certain extent (reference 8).

Form resistance does not contribute directly to heat diffusion, although very high heat transfer has been ascertained on the back of pipes in oblique flow especially at large Reynolds numbers, which are traceable to such vortices. Up to the present no theoretical formula has been published for this type of heat transfer (reference 2, p. 150). The induced drag on the wing is, in this sense, equally to be treated as form drag, that is, it may affect the boundary layer flow very slightly.

The heat transfer on the nose of the airfoil is most easily comparable with that on the pipe in oblique flow, but it is just as difficult to treat theoretically as that on the front of a pipe. However, the following holds true:

a) The heat dissipation of a surface area is so much greater as it is closer to the stagnation point;

b) It varies in relation to the angle of attack and the Reynolds number similar to the dissipation of the side of the wing of which it occupies the major portion;

c) The smaller the heat dissipating area near the stagnation point is, the greater its heat dissipation will be and so much less its dependence on the angle of attack. Fairly small areas fall within the laminar region (approximately $Rex < 10^4$); hence Nux varies very slowly with the Reynolds number (with $Rex^{1/2}$).

With exception of the tests on the heat dissipation of wing radiators, described in R.&M. Report No. 1163, only mean values for the Nusselt number are known. But within the framework of the necessary experimental data the distribution of heat dissipation along the outer skin of the surface by constant limitation of the skin radiator is of particular interest, because the local cooling conditions and the heat stresses are governed by it. If the analogy between flat plates and airfoils can be extended, the local values of heat-transfer coefficients can be closely approximated in power form $Nux = M Rex^N$ from the measured mean values by differentiation of the empirical data, analogous to the function represented in equation (19), at least for the case where the heating extends without interruption from the leading edge up to depth x. After that, it is important to

know the appropriate areas on the wing surface for the heat dissipation in order to be able to find the best arrangement for the particular case.

For the heat dissipation of partial surfaces the statements made concerning the flat plate hold true. For every chosen parameter x_1/x a factor w is computed similar to equation (22), with reference to the proper Nux_T or Nux_L; w, which again can be a function of Rex, might at the same time include the temperature effect. Accordingly, it will be advisable to use the relations governing the flat plate — extrapolated to increase of temperature $\Theta = 0$ — as "standard" for a basis in form of the curves Nux_L, Nux_T, and $Nux_{\ddot U}$. The actual variation must, of course, be established by very careful experiments, while the concept "transitional region" requires a more exact interpretation. Comparison might also be made with a "standard function" for which Nux_K is probably most suitable, since it is free from empirically defined values. For reduction to other temperature ranges the previously introduced mean value for Pr should be retained and the variation of Pr in the expression V allowed for.

Irrespective of what new information is obtained for practical calculations the representation according to figure 1 should even then be more convenient than that according to figure 6, if the temperature effect is included in the suggested form.

VII. SUPPLEMENTARY DRAG OF SKIN RADIATORS

The transition from the speed of undisturbed flow to zero value of the gas particles adhering to the surface takes place, as is known, within the boundary layer. In accord with measurements we chiefly differentiate between the parabolic velocity distribution in the laminar boundary layer and the distribution in the turbulent boundary layer according to the 1/7 power law (pt. IV). If the temperature of the surface differs from that of the gas, the statements concerning the temperature variation in the boundary layer hold true. If the relation of density ρ, kinematic viscosity v, and temperature conductivity a to air temperature is discounted, the fields of velocity

and temperature are exactly similar for the specific case
that friction and heat dissipation begin simultaneously
and the Prandtl number is equal to 1, the increase of
temperature being computed from the surface temperature
T_0. Many problems can be satisfactorily solved with the
aid of this simple, although not exactly correct rela-
tionship. For more accurate adaptation to practice the
previously cited values ψ and φ deduced from tests
we used.

The nature of the temperature effect on the drag con-
sists, accordingly, in the simultaneous influence on the
boundary layer thickness and further on the velocity pro-
file within the boundary layer. In the test the two ef-
fects can, of course, be measured only concurrently.
Application to geometrically similar processes is very
reliably possible if the critical values are borne in mind.
But it first needs to be proved that the data on the drag
of thin, heated plates is applicable to airfoils; the ef-
fect on the boundary layer thickness being treated as if
it did not change the velocity distribution within the
boundary layer.

It may be suspected that with regard to drag a heated
airfoil is decidedly thicker by $\Sigma\Delta\epsilon$ than the cold one,
and the conversion of the thereby increased flow veloci-
ties to pressure could favor the formation of further form
drag. Owing to the variation of the increases of velocity
past the curved surface the boundary layer will form some-
what different from that of a flat plate but the discrep-
ancies are small. (Cf. pt. V.) Undoubtedly the form drag
(local vortices) is also of some influence.

In order to make the estimation of the hypothetical
thickening clear, an airfoil with vanishing form drag but
finite skin friction is investigated, in its effect on a
potential flow, first cold, then heated to temperature in-
crease Θ. By assumption of the decisive velocities v_x for
both surfaces of the wing the boundary layer thickness on
all points of the airfoil circumference is (reference 2,
pp. 138-139).

$$\frac{\delta}{x} = 5.477 \, Re_x^{-0.5} \quad \text{For } \textbf{laminar} \text{ boundary layer} \qquad (28)$$

$$\frac{\delta}{x} = 0.37 \, Re_x^{-0.2} \quad \text{For turbulent boundary layer} \qquad (29)$$

An airfoil without skin friction — that is, on which the potential flow remained up to the surface would, at equal pressure — and hence, velocity distribution, have to be just as much thicker as the boundary layer thickness decreased, if the potential velocity v_x prevailed in it. For the thickness δ' of the substitute layer — if y in figure 8 is the distance of a filament from the surface within the boundary layer — must be

$$\rho u \delta' = \int_0^\delta \rho v_{xy} \, dy$$

According to general law of velocity distribution

$$\frac{v_{xy}}{v_x} = \left(\frac{y}{\delta}\right)^m$$

where $m = 1/2$ for laminar, and $m = 1/7$ for turbulent boundary layer, we get

$$\left.\begin{aligned}
\delta' &= \frac{1}{1 + m}\ \delta \\[2ex]
\delta - \delta' &= = \frac{m}{1 + m}\ \delta
\end{aligned}\right\} \tag{30}$$

The new profile obtained on this basis, which similar to the so-called half-body extends to infinity, can of course, never exactly fulfill the theoretical condition for zero skin friction (sum of all pressure forces equal zero) because of the already mentioned simplifications, and particularly, because the potential velocity v_x is not quite reached on the "outer limit" of the boundary layer.

On the heated profile the boundary layer thickens up as a result of the heat expansion. Since no appreciable acceleration forces can occur in flow direction by reason of the small inclination of the outside limitation of the boundary layer toward the surface, it may be assumed that each infinitely small width dy expands almost exactly in correspondence with its temperature. Hence, according to figure 8:

$$\delta_{\Theta} = \int\limits_{0}^{\delta} dy \; \frac{T_y}{T}$$

$$T_y = T_0 - \Theta \left(\frac{y}{\delta} \right)^m$$

$$\delta_{\Theta} = \frac{T_0}{T} \delta - \frac{1}{1 + m} \frac{\Theta}{T} \delta = \left(1 + \frac{m}{1 + m} \frac{\Theta}{T} \right) \delta$$

The substitute thickness δ_{Θ}' for the boundary layer converted for the potential velocity v_x follows from

$$
\left.
\begin{aligned}
\rho \, v \, \delta_{\Theta}' &= \int\limits_{0}^{\delta} \rho_y \; v_{xy} \left(dy \, \frac{T_y}{T} \right) \\[2mm]
&= \int\limits_{0}^{\delta} \rho \, \frac{T}{T_y} \, v_{xy} \, \frac{T_y}{T} \, dy \\[2mm]
&= \int\limits_{0}^{\delta} \rho \, v_{xy} \, dy \\[2mm]
\delta_{\Theta}' &= \frac{1}{1 + m} \, \delta \; (= \delta')
\end{aligned}
\right\}
\qquad (31)
$$

To transform the actual profile in a "equivalent" profile without skin friction it must be thickened at all points by ϵ_{Θ} or, compared to the cold one, by $\Delta \epsilon$.

According to equations (31) and (30) and figure 8:

$$\Delta \epsilon = \epsilon_{\Theta} - \epsilon = \frac{m}{1 + m} \frac{\Theta}{T} \delta \qquad (32)$$

For the general case of a profile with finite form drag this argument holds true at least in its tendency. Hence the following conclusion: for the flow past the profile the latter on heating — as compared to cold — seems to be thicker by the sum of the quantities $\Delta \epsilon$ for the two profile surfaces. Hence, with equation (28):

$$\Sigma \Delta \epsilon = \Sigma \; \frac{1}{3} \; \frac{\Theta}{T} \; 5.477 \; Rex^{-0.5} \; x \quad \text{For laminar boundary layer} \quad (33)$$

with equation (29)

$$\Sigma \Delta \epsilon = \Sigma \; \frac{1}{8} \; \frac{\Theta}{T} \; 0.37 \; Rex^{-0.2} \; x \quad \text{For turbulent boundary layer} \quad (34)$$

The inferior accuracy of equation (32) justifies, for simplification, the introduction of the undisturbed velocity v in place of the decisive velocities v even at greater angles of setting and a mean value instead of the arc lengths x computed for both wing surfaces from the stagnation point to the point of maximum profile thickness. Lastly, it is assumed that the distance of the point of maximum profile thickness is about 30 percent of the chord length t from the wing leading edge. Since the profile circumference is slightly greater than $2t$ it is approximately

$$Rex = 0.15 \; Re$$

$$x = 0.3 \, t$$

The thickening $\Sigma \Delta \epsilon$ is referred to the actual maximum profile thickness d itself:

$$Vd = \frac{\Sigma \Delta \epsilon}{d}$$

Then the equation for the laminar boundary layer, (32) reads:

$$\left. \begin{aligned} V_{dL} &\sim 2 \; \frac{1}{3} \; \frac{\Theta}{t} \; 5.477 \; (0.15 Re)^{-0.5} \; 0.3 \; \frac{t}{d} \\ V_{dL} &\sim 2.8 \; \frac{t}{d} \; Re^{-0.5} \; \frac{\Theta}{T} \end{aligned} \right\} \quad (35)$$

and for the turbulent boundary layer, equation (34):

$$\left. \begin{aligned} V_{dT} &\sim 2 \; \frac{1}{8} \; \frac{\Theta}{t} \; 0.37 \; (0.15 \; Re)^{-0.2} \; 0.3 \frac{t}{d} \\ V_{dT} &\sim 0.041 \frac{t}{d} \; Re^{-0.2} \; \frac{\Theta}{T} \end{aligned} \right\} \quad (36)$$

Equation (35) will serve for small models, equation (36) for full-scale versions. In all practical cases the amounts of V_d lie at 1 percent,* hence the form drag is scarcely affected by the heating in normal flight attitudes. Therefore the test data on flat plates can be applied fairly reliably to airfoils. In this connection it is further of interest to know whether portions of the heated outer skin lower the lift of the profile, especially its maximum, and whether the flow is adversely affected, so as to induce earlier breakaway than on the unheated wing with increasing angle of setting. Such phenomena are said to have been observed in past experiments and they appear altogether plausible according to the foregoing arguments, even though these do no longer permit of safe conclusions in these extreme cases. If the flow still adhers on the cold wing the assumed slight thickening up of the profile due to heating may very well be sufficient to make it separate.

Despite the fact that Ten Bosch's method appears to make the temperature effect excessive, the lack of other data prompts its use for determing the skin friction on a thin, flat plate heated over its total length to uniform increase of temperature Θ and surface temperature T_0 in two-dimensional flow. This merely involves the conversion of Re_x to Re_{x_0} by means of equation (27) and insertion in C_f along with the still unknown factor ξ, the numerical values of which are taken from pipe flow. The ratio of resistance of the heated to the cold plate

$$V_c = \frac{C_{f\Theta}}{C_f}$$

a)
$$V_{CL} = \xi \left(\frac{T\eta}{T_0\eta_0} \right)^{-0.5} \tag{37}$$

for "short" plates (predominately laminar boundary layer, $Re_{x_0} < Re_{x_{cr}}$) according to equation (11).

b)
$$V_{CU} = \xi \tag{38}$$

for "medium" plates, (largely transitional boundary layer, $Re_{x_{cr}} << Re_{x_0} < 2 \times 10^7$) according to equation (14)

---

*For the small model cited in the subsequent footnote, we get in round numbers $Re \sim 0.7 \times 10^6$ ($v \sim 20$ m/s, as minimun value), $\Theta \sim 75°$, $T \sim 298°$, $d/t \sim 0.13$. According to equation (35) $V_{dL} = \sim 0.01$ (1 percent). If $Re \sim 10^7$, $\Theta \sim 100°$, $T \sim 223°$, $d/t \sim 0.13$. Equation (36) gives $V_{dT} = \sim 0.01$ (1 percent).

c) $$V_{OT} = \xi \left(\frac{T\eta}{T_0 \eta_0} \right)^{-0.2}$$ (39)

for "long" plates (predominately fully turbulent boundary layer, $Rex \gg 2 \times 10^7$) according to equation (16).

With the approximated relation $\frac{\eta}{\eta_0} = \left(\frac{T}{T_0} \right)^{0.5}$. these facts become even more evident.

The evaluation of equations (37), (38), and (39) is graphically represented in figure 9. On the basis of the little reliable assumptions made, it is found that: on short plates the skin friction drag rises with ascending Θ but slower for high temperatures, with an initial drag decrease at low Θ; the same holds for long plates, but the initial decrease is more distinct, and the curve is subsequently flatter. On medium plates, on the other hand, the frictional drag drops to a minimum value, with ascending Θ, independent of the actual height of temperature.*

If the fore part of a plate is not heated, its skin friction drag naturally decreases proportionally less than corresponds to the ratio of the heat volumes (factor w). The exact magnitude of the frictional force exerted by the flow through the heated boundary layer onto a cold portion disposed behind the heated surface must be decided by experiment. Numerically this proportion of the drag lies naturally between that occurring in isothermic flow, if the temperature is, once T, then T_0.

---

*The heat dissipation of surface portions distributed over the nose, upper and lower surface to the amount of ~55 percent of the profile circumference was measured on a model wing, heatable to 250 millimeters chord (O. Seibert, Jahrbuch 1938 der deutschen Luftfahrtforschung, pp. II 224 – II 244). Subsequent drag measurements, by O. Schoppe, disclosed as definite increase in the total drag on heating throughout the entire possible range (Re to ~2×10^6).
The average for Vc was 1.12 at to ~100^0; t ~25^0 (Θ ~75^0). The proportion of the laminar flow to the skin friction was certainly still perceptible on the model. Greater geometrical similarity would have perhaps afforded a lower V_c at these temperatures.

On a wing with heating surfaces in the foreward portion
only, the pressure distribution measurement in the rear
unheated portion which can be easily made during the heat
transfer experiments, itself is likely to afford practical
data for the evaluation of the flow and separation phe-
nomena.

Impending measurements may yield smaller drag varia-
tions than those deduced. But in any event the tenden-
cies will hold good to some extent. Perhaps this dis-
similarily in behavior of plates or airfoils depending
upon the momentary Reynolds number enables an explanation
of several contradictory observations on the relationship
between drag and temperature.

Translation by J. Vanier,
National Advisory Committee
for Aeronautics.

---

*(Continued from p. 29) Figure 9 shows V_c at about 1.06
for the cited conditions. If the finite Θ were exactly
allowed for, it would have had to result in a value higher
than that recorded, since completely heated surface had
been assumed for the study and the temperature effect was

known to be too great. The term $\left(\dfrac{T_\eta}{T_o T_\eta}\right)^{-0.5}$ is with

1.22 actually greater than the test value V_o. This seems
to suggest that the unknown factor ξ is considerably
closer to 1 for flat plates and airfoils than for the flow
in pipes.

REFERENCES

1. Elias, F.: The Transference of Heat from a Hot Plate
      to an Air Stream. T.M. No. 614, NACA, 1931.

2. Ten Bosch, M.: Die Wärmeübertragung. Julius Springer
      (Berlin), 1936, pp. 136-148.

3. Von Kármán, Th.: Über laminare und turbulente Reibung.
      Z.f.a.M.M., Bd. 1, 1921, pp. 233-252.

4. Latzko, H.: Der Wärmeübergang an einen turbulenten
      Flüssig-keits- oder Gasstrom, ebenda. pp. 268-290.

5. Reynolds, O.: Sci. Pap., vol. 2, Cambridge, Univ.
      Press. 1901.

6. Prandtl, L.: Zur turbulenten Strömung in Rohren und
      längs Platten. Ergebnisse der Aerodynamischen Ver-
      suchsanstalt Göttingen, IV. Lieferung, pp. 18-19,
      R. Oldenbourg (Munich and Berlin); dasselbe für
      Tragflugel s. z. B. Fuchs-Hopf-Seewald, Aerodynamik
      Bd. I, Julius Springer (Berlin), 1934.

7. Gutsche, F.: Der Kennwerteinfluss beim Modellversuch
      des Wasser- und Luftfahrzeuges. Z.V.D.I., Bd. 77
      1933, p. 1255.

8. Hermann, R.: Wärmeübergang bei freier Strömung am
      waagerechten Zylinder in zweiatomigen Gasen.
      Forsch. Ing. Wes., Heft 379, (Berlin), 1936, VDI-
      Verlag.
   Jung, I.: Wärmeübergang und Reibungswiderstand bei
      Gasströmung in Rohren bei hohen Geschwindigkeiten
      Forsch. Ing. Wes., Heft 380, (Berlin), 1936, VDI-
      Verlag.
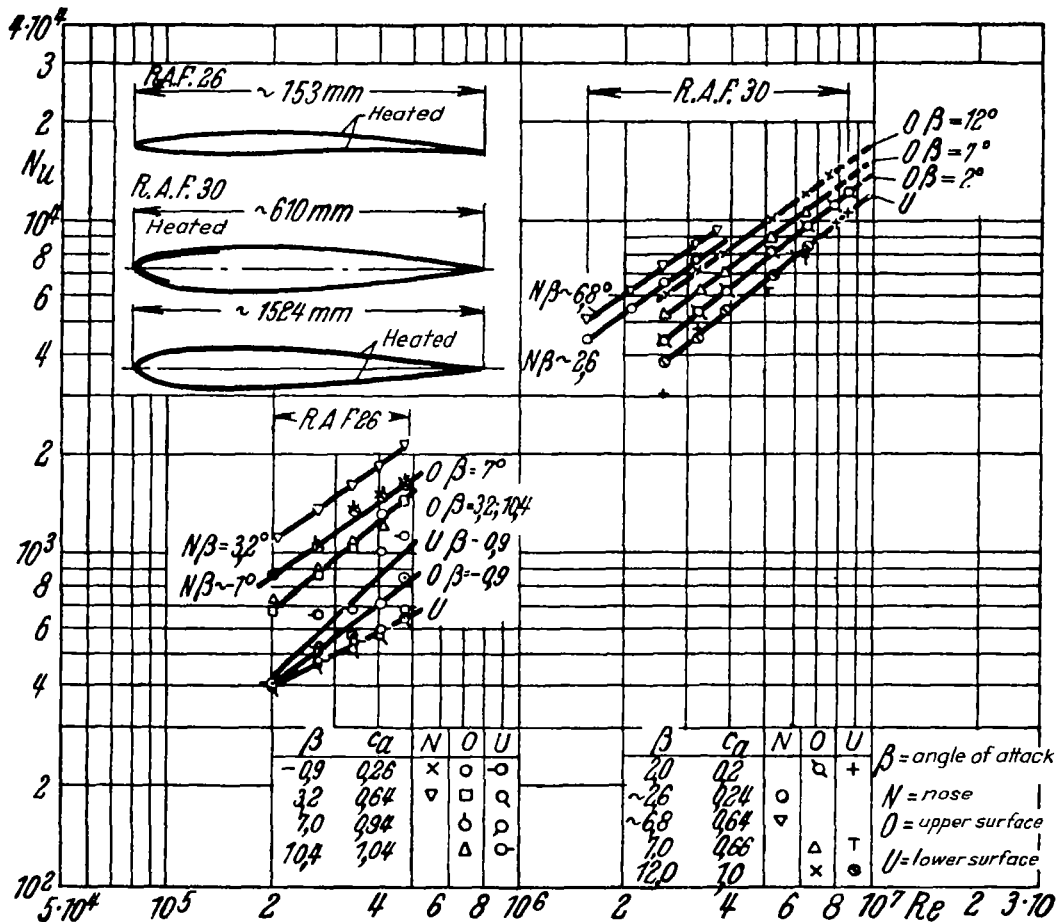
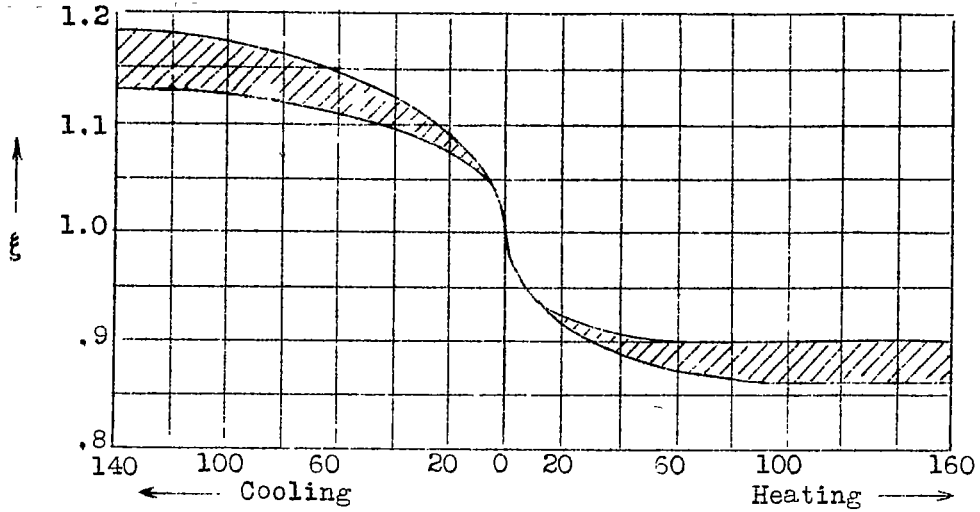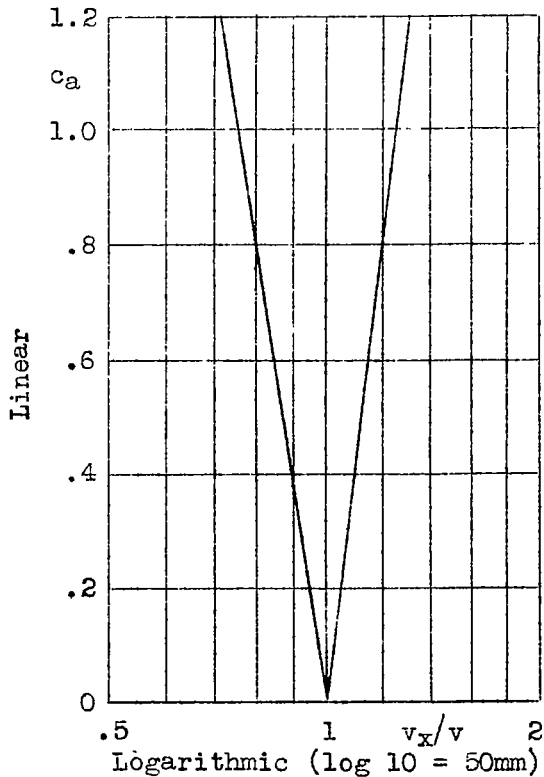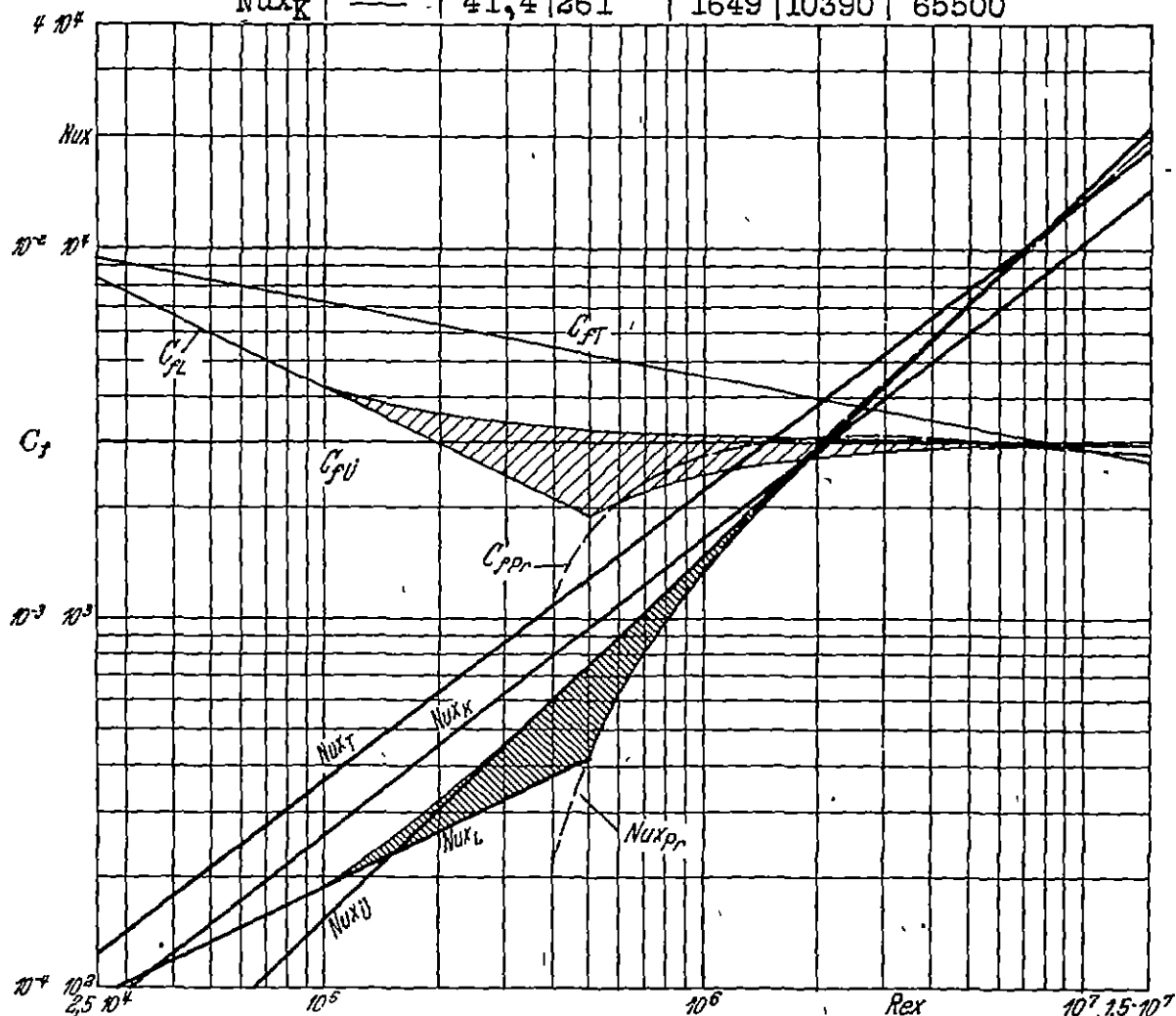Figure 1.— Representation of $Nu = f(Re)$ according to R and M Reports 1163, 1311, 1326, and 1481.

Figure 2.- ξ values for air.

Figure 5.-
v_x/v (for cos
ϑ-1) total
plate plotted
against c_a
(according to
equation 24).

Evaluation of equation (19)

Rex	10^3	10^4	10^5	10^6	10^7	10^8
Nux_L	18,86	59,7	188,6	597	——	——
Nux_U	——	15,6	151,1	1461	14130	136800
Nux_T	——	59,6	364	2220	13540	82600
Nux_K	——	41,4	261	1649	10390	65500

Subscripts:
L = laminar boundary layer
U = transitional region
Pr = (according to Prandtl)
T = turbulent boundary layer
K = (according to Kármán-Latzke)

Figure 3.— Relation of drag coefficients C_f and the mean Nusselt
number Nux for the flat plate with the Reynolds
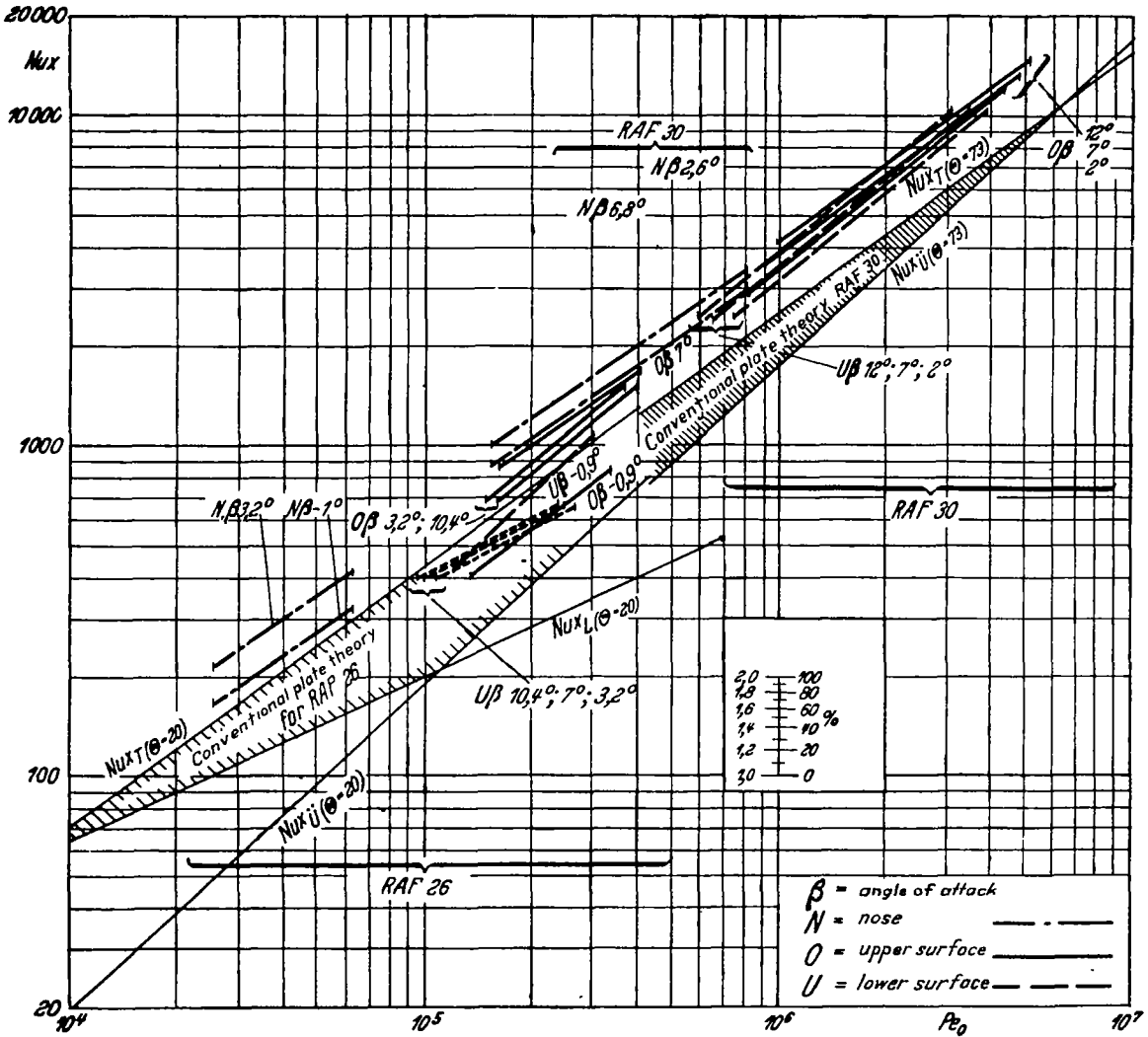number (increase of temperature = o).
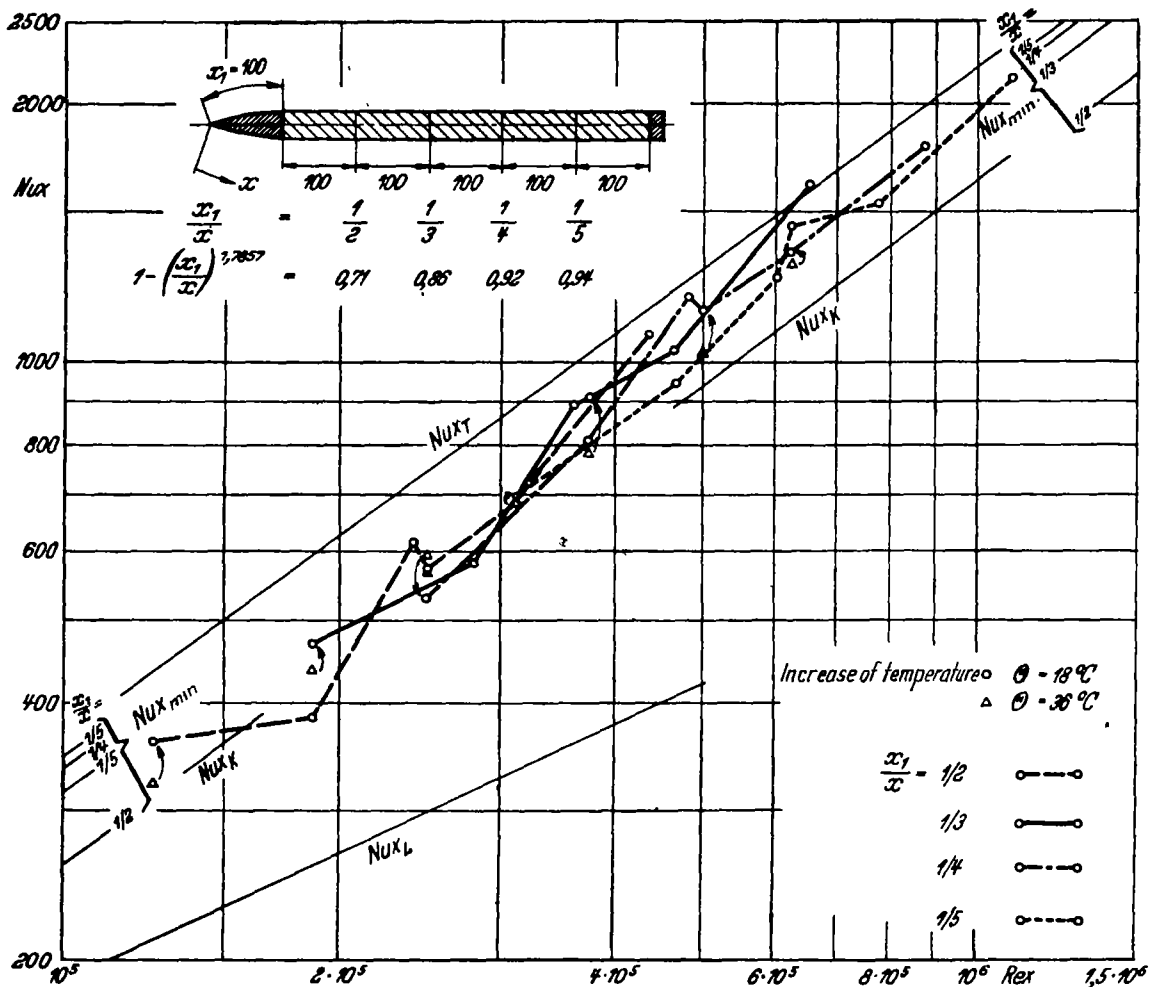
Figure 4.- Comparison of the theoretical relation Nux and
Rex of the flat plate with Elias' test data

$\dfrac{x_1}{x} = \dfrac{\text{depth of cold fore portion}}{\text{depth of total plate}}$
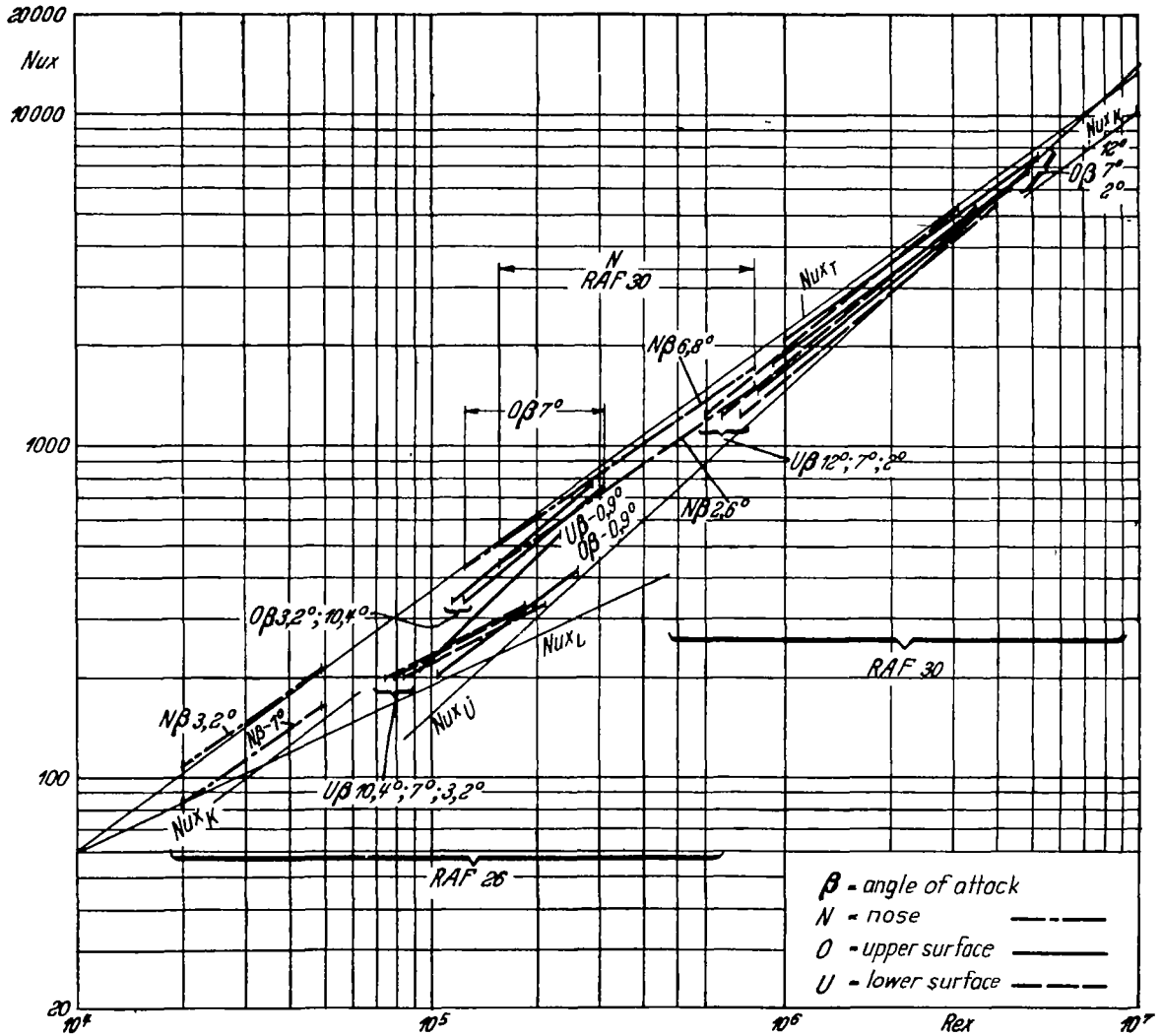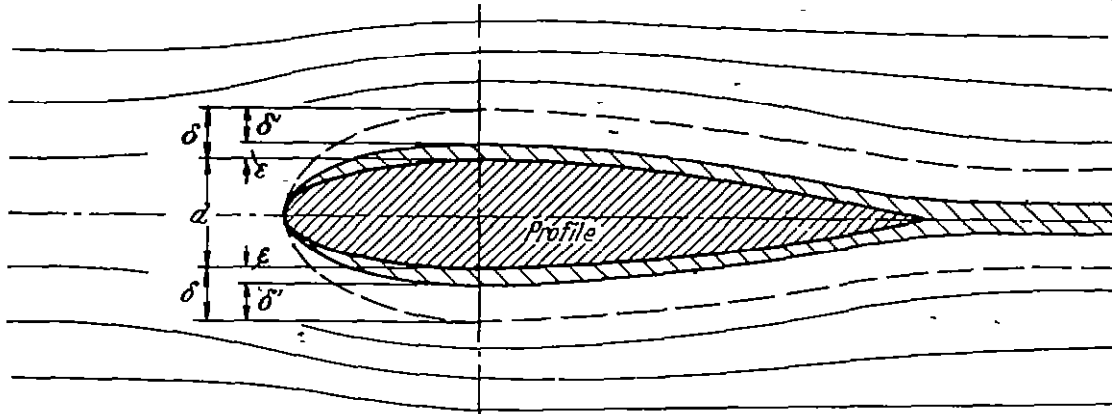
Surface temperatures
RAF 26   ∼   40°C
RAF 30   ∼   93°C
Flat plate = air
    temperature ∼ 20°C

Figure 6.— Reduced actual Nux plotted against the theoretical
        Nux for the flat plate.

RAF 26θ = 20°
RAF 30θ = 73°

Figure 7. Figure 6 replotted against Pe_θ to allow for the temperature effect according to ten Bosch (surface temperature of flat plate the same as that of models).

$$\epsilon = \delta - \delta',$$
$$\epsilon_\theta = \delta_\theta - \delta_\theta',$$
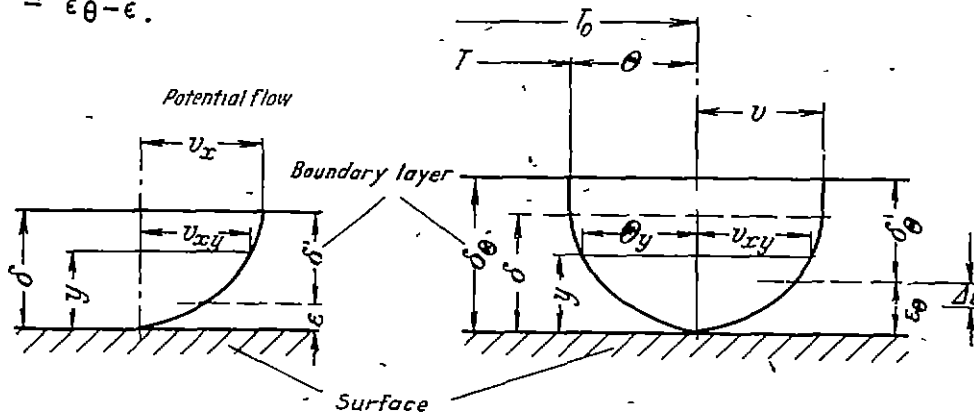$$\Delta\epsilon = \epsilon_\theta - \epsilon.$$

Figure 8.— Effect of heating on the flow,
$\delta; \delta_\theta$ = actual boundary layer thickness
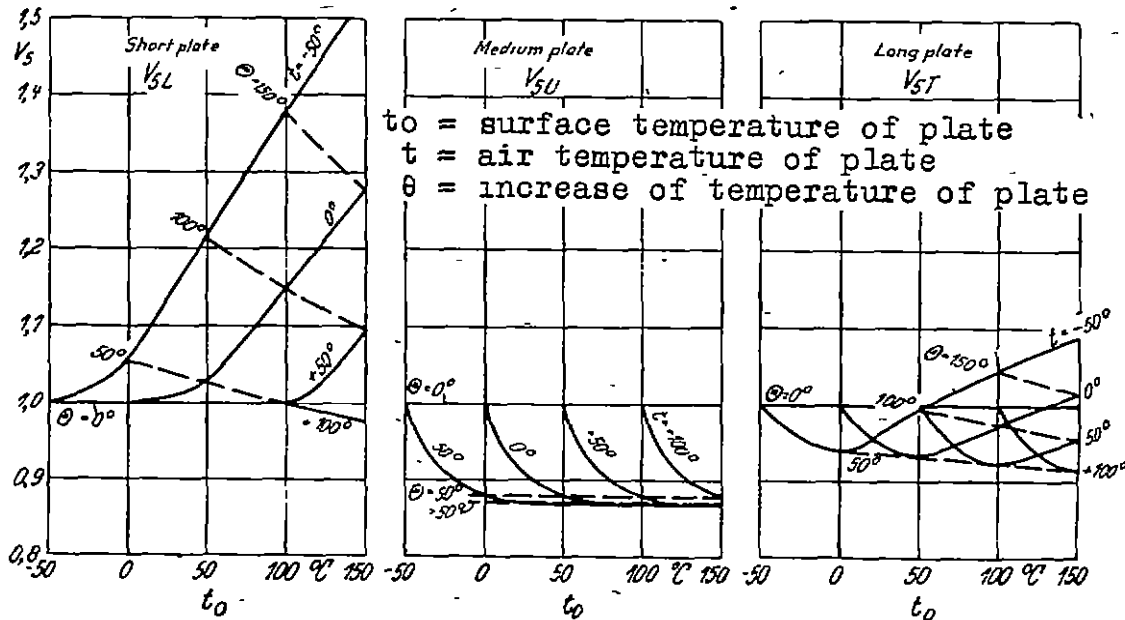$\delta'; \delta_\theta'$ = substitute thickness

to = surface temperature of plate
t = air temperature of plate
θ = increase of temperature of plate

Figure 9.— Drag variation of plate due to heating = Vc
(assumptions)